Local instability of the MnF_8 complex in BaF_2 studied by ENDOR

1992 J. Phys.: Condens. Matter 4 7927

(http://iopscience.iop.org/0953-8984/4/39/008)

J. Phys.: Condens. Matter 4 (1992) 7927–7936. Printed in the UK

Local instability of the MnF_8 complex in BaF_2 studied by ENDOR †

H Soethe, V A Vetrov¶ and J-M Spaeth

Department of Physics, University of Paderborn, Warburger Strasse 100, 4790 Paderborn, Federal Republic of Germany

Received 1 July 1992

Abstract. The structural change of the nearest neighbourhood of eight fluorines surrounding Mn^{2+} in BaF_2 from a cube to two sets of tetrahedra at low temperatures has been shown to occur by ENDOR measurements. The angular dependence of the ENDOR lines of the eight nearest neighbours and a characteristic splitting of the ENDOR lines of the second shell rule out other possibile ways of explaining the former EPR results. The temperature dependence of the spectra points to a dynamic process causing the structural transition observed

1. Introduction

In the electron paramagnetic resonance (EPR) spectra of Mn^{2+} in BaF_2 an unusual temperature effect had been observed (Badalyan *et al* 1986) consisting in a drastic change of the superhyperfine (SHF) structure of the EPR spectrum between 45 und 50 K. For the magnetic field along the cubic crystal axis above 50 K it consists of six hyperfine (HF) lines of ^{55}Mn ($I = 5/2$), each of which is split into nine SHF lines with the intensity ratio one expects for the SHF interaction with eight equivalent ^{19}F ($I = 1/2$) nearest neighbours if Mn^{2+} substitutes for Ba^{2+}. There is no apparent fine-structure splitting as expected for cubic symmetry. However, upon cooling to 45 K the SHF structure changes drastically into a much more complicated pattern (see figure 1), while the ^{55}Mn structure remains unchanged. This has been explained by a local change in the lattice geometry of the eight nearest neighbours. Four tetrahedrally arranged fluorines were thought to move along ⟨111⟩ towards the unshifted manganese ion, the other four to move away along ⟨111⟩ directions. The resulting SHF structure for the magnetic field along [100] is close to the 17-line pattern with relative intensities of 1:4:6:8:17:24:22:28:36:28:22:24:17:8:6:4:1, predicted in this model when assuming the ratio of the SHF interactions of each of the tetrahedral shells to be approximately 3:1. In figure 2(*a*) this is shown only for one of the six ^{55}Mn HF groups. For this orientation the four ^{19}F ligands closest to the Mn^{2+} ion are equivalent, causing a 1:4:6:4:1 spectrum with each component again split into 1:4:6:4:1 lines by the interaction with the other four equivalent 'outer' ^{19}F ligands resulting in a 25-line SHF structure. Assuming a 3:1 ratio for the SHF constants of both tetrahedral

† Dedicated to A Scharmann on the occasion of his 65th birthday.

¶ Permanent address: A F Ioffe Institute, St Petersburg, Russia.

0953-8984/92/397927+10$04.50

groups, 16 of the total number of 25 resonances overlap, so that a 17-line pattern is observed. A more thorough inspection reveals, however, that more than 17 lines are present. This becomes especially apparent in the outer ^{55}Mn HF components (see figure 1). Since it is practically impossible to determine the angular dependence of the SHF structure of the EPR with sufficient precision, some uncertainties remained with respect to the model proposed for the structural change. Mn^{2+} could go off-centre and change its cubic field-splitting parameter, which would also result in a complicated EPR structure. The EPR spectrum of a second type of Mn^{2+} centre could also appear when the temperature was lowered, causing a complicated superposition of spectra.

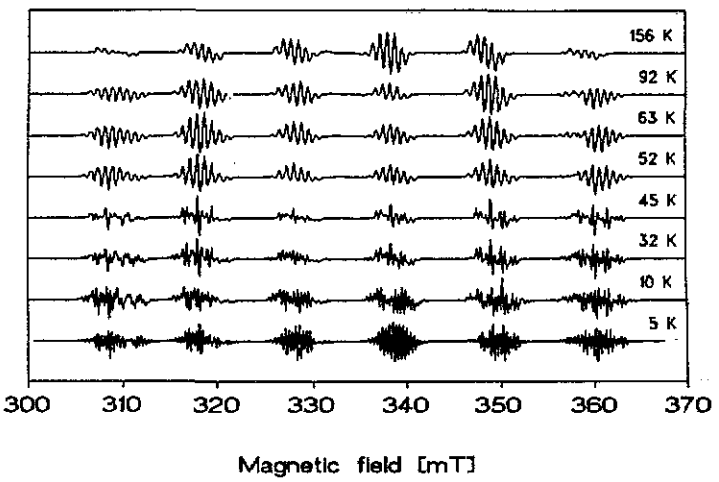

Figure 1. Temperature dependence of the X-band EPR spectrum of Mn^{2+} in BaF_2, with magnetic field along [100].

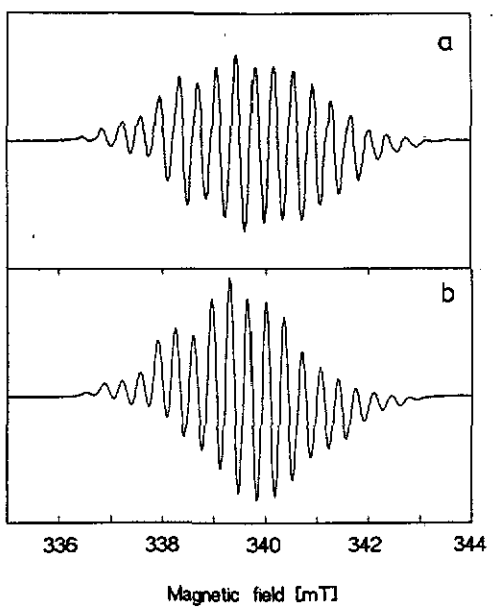

Figure 2. (*a*) Experimental fluorine SHF structure of the $m_I = 1/2$ ^{55}Mn HF line at $T = 5$ K for $H_0 \parallel [100]$, (*b*) simulation of the fluorine SHF structure of the $m_I = 1/2$ ^{55}Mn HF line at $T = 5$ K for $H_0 \parallel [100]$.

With electron nuclear double resonance (ENDOR) the SHF interactions can be resolved with higher precision and one can hope to resolve also those of farther ligand shells, which would help to establish whether the proposed local structural instability does indeed exist around Mn^{2+} occupying Ba^{2+} sites in BaF_2. We performed an ENDOR investigation of this defect system as a function of temperature and could show that the originally proposed explanation by Badalyan *et al* (1986) for the temperature change of the SHF structure was correct. Our results point to dynamical processes causing the structural changes.

2. Experimental procedure

Crystals for this investigation were BaF_2 single crystals doped with 20 ppm to 1% Mn^{2+} in the melt, grown in the crystal growth laboratory of the University of Paderborn and in Leningrad. For the EPR and ENDOR measurements a computer controlled custom built spectrometer (X-band) allowing measurements between 4.2 and 300K was used at the University of Paderborn; some measurements were conducted at the University of Giessen on an AEG 20XT spectrometer equipped with a Bruker ENDOR cavity.

3. Analysis of EPR and ENDOR spectra

The magnetic resonance spectra of Mn^{2+} in the cubic fluorites can be described by the spin Hamiltonian (Richardson *et al* 1971)

$$\mathcal{H} = g\beta \boldsymbol{H}\boldsymbol{S} + \tfrac{1}{6}a\,(S_x^4 + S_y^4 + S_z^4 - \tfrac{707}{16}) + \boldsymbol{A}\boldsymbol{S}\boldsymbol{I} + \sum_{i=1}^{n}(\boldsymbol{S}\tilde{T}_i\boldsymbol{I}_i - \gamma \boldsymbol{H}\boldsymbol{I}_i) \tag{1}$$

representing the Zeeman and cubic field energies of the $^6S_{5/2}$ electronic ground state, the isotropic hyperfine (HF) interaction with the ^{55}Mn nucleus ($I = 5/2$, 100% abundance), the SHF interactions with the ^{19}F ligands ($I = 1/2$, 100% abundance) and their nuclear Zeeman interactions (γ is the gyromagnetic ratio of ^{19}F). The $\Delta m_S = \pm 1, \Delta m_I = 0$ transitions occur in the magnetic fields

$$H = H_0 - \tfrac{1}{64}a f(\Theta, m_S) - A m_I - \frac{A^2}{2H}\left[\tfrac{35}{4} - m_I^2 + m_I(2m_S - 1)\right]$$
$$- \frac{A^3}{2H^2}\left\{(2m_S - 1)(\tfrac{35}{4} - 3m_I^2) - m_I(\tfrac{31}{2} - m_I^2) + 3m_I m_S(m_S - 1)\right\} \tag{2}$$

where the angle Θ represents the orientation of the magnetic field with respect to the cubic field coordinate system. This third-order calculation yields a small splitting of the six dominating HF lines even if the cubic field-splitting parameter a is zero (as is usually observed in fluorites). There is then a splitting into numerous SHF lines. It is thus difficult to decide whether the observed temperature effect on the EPR line pattern is caused by a change in the cubic field splitting, by the appearance of a second type of Mn^{2+} centre which is measurable only at sufficiently low temperatures

due to a short spin–lattice relaxation time or, as proposed by Badalyan *et al*, by a change of the SHF term of the nearest neighbours from one sum over eight equivalent ligands to two sums with four equivalent ligands each but with different SHF tensors.

The ENDOR frequencies resulting from the transitions $\Delta m_S = 0$, $\Delta m_I = \pm 1$ of the spin Hamiltonian are given by (see e.g. Richardson *et al* 1971)

$$\nu_{\mathrm{ENDOR}} = \{Q^2(m_S) + [P^2(m_S) - Q^2(m_S)]\cos^2\vartheta_i\}^{1/2} \tag{3}$$

where ϑ_i is the angle between the magnetic field direction and the axis connecting Mn^{2+} with the ligand i; this is the principal axis of the axial ^{19}F SHF tensor for a cubic or tetrahedral ^{19}F neighbourhood of Mn^{2+}. In first-order perturbation theory one obtains

$$P(m_S) = T_\parallel m_S - \nu_F \qquad Q(m_S) = T_\perp m_S - \nu_F \tag{4}$$

where $T_\parallel$ and $T_\perp$ are the components of the axial SHF tensor and ν_F is the Larmor frequency of the ^{19}F nuclei, $\nu_F = g_N\beta_N H$. With corrections of second and third order they become (Zaripov *et al* 1975)

$$P(m_S, m_I) = \left(m_S + \frac{A^2[m_I S(S+1) - m_S I(I+1) - m_S m_I(m_S+1)]}{2(g\beta H)^2}\right)T_\parallel - \nu_F - \frac{S(S+1) - m_S^2}{2g\beta H}T_\perp^2 \tag{5a}$$

$$Q(m_S, m_I) = \left(m_S + \frac{A^2[m_I S(S+1) - m_S I(I+1) - m_S m_I(m_S+1)]}{2(g\beta H)^2}\right)T_\perp - \nu_F - \frac{S(S+1) - m_S^2}{2g\beta H}T_\parallel T_\perp. \tag{5b}$$

4. Experimental results

The ENDOR angular dependence measured at $T = 5$K in the (110) plane for the $m_I = 1/2$ group of Mn^{2+} is shown in figures 3(*a*) and 3(*b*). The angular dependencies found for the ^{19}F ENDOR lines are typical for ligands which have a '(111) symmetry', i.e. the principal axes of their axial SHF tensors point along ⟨111⟩ directions. This is what is expected for eight ^{19}F neighbours on the eight corners of a cube. For a rotation in a {110} plane there are one set of four and two sets of two ligands which remain equivalent, i.e. have the same angles ϑ_i and thus the same SHF interactions. This results in three branches of ENDOR lines for each value of m_S, which coincide for $H_0 \parallel [100]$. Slight deviations from the coincidence are due to a small misalignment of the sample. Small 'doublet splittings' of the first-shell ENDOR lines are also due to this misalignment: the equivalence of some ligands is broken. The solid lines in figure 3(*a*) represent the angular dependence calculated with equations (3) and (5) using $T_\parallel = 43.98$MHz and $T_\perp = 21.92$MHz. The $m_S = -1/2$, $3/2$, $-3/2$ (and one branch of 5/2) ENDOR lines are identified. However, the calculated angular dependence does not describe all measured ^{19}F ENDOR lines. For example, another three-branch group of ENDOR lines is observed

around 18 MHz, which has the same type of angular dependence. The lines are due to another set of ^{19}F ligands with (111) symmetry (yet with a different SHF tensor). Figure 3(*b*) shows the measured spectra again and the calculated angular dependence for $T_{\parallel} = 19.49$ MHz, $T_{\perp} = 4.23$ MHz and $m_S = -1/2, -3/2$ and $-5/2$. With the two SHF tensors and (111) symmetry, all ENDOR lines found above 16 MHz can be explained. Thus, the ENDOR angular dependence reveals two different shells of ⟨111⟩ ligands. The number of nuclei in each shell cannot be inferred from the ENDOR analysis. This can be done, however, using the EPR spectrum. In agreement with the analysis of Badalyan *et al* (1986), there must be two sets of four tetrahedral ^{19}F nuclei, one with a larger and one with a smaller SHF interaction. We will refer to the former as the 'short bond' and to the latter as the 'long bond' ligands. The characteristics of the three-branch angular dependence is the same as for a tetrahedral or cubic environment, except that the number of nuclei is halved in the tetrahedral one.

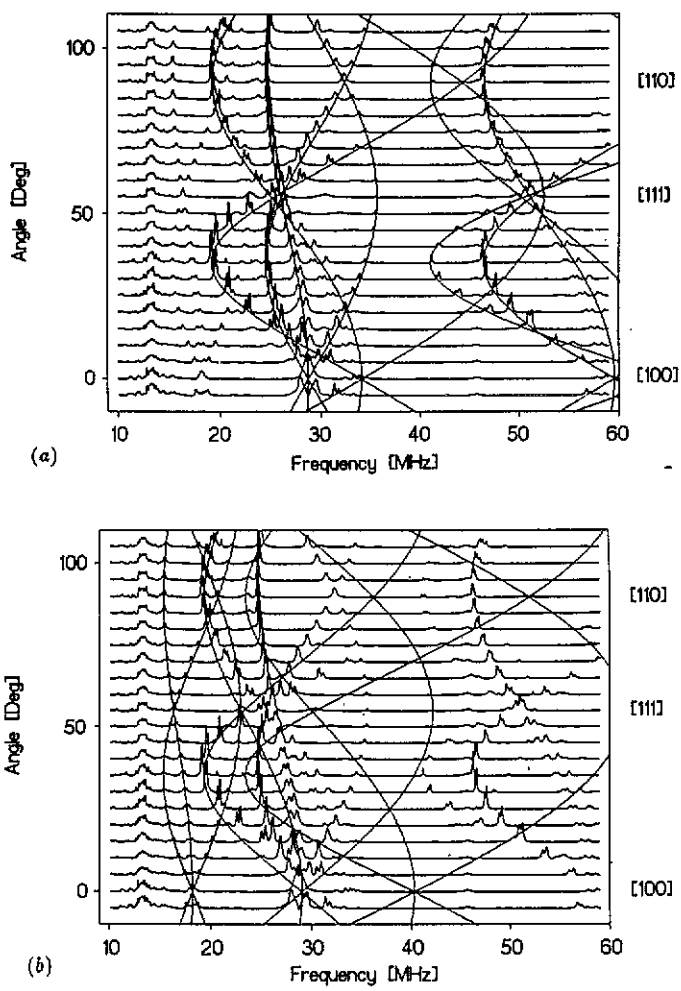

Figure 3. Angular dependence of ^{19}F ENDOR lines for rotation of the magnetic field in a {110} plane, $H_0 = 339$ mT (set into the ^{55}Mn $m_I = 1/2$ HF group), $T = 5$ K. The solid lines are calculated using equations (3) and (5) for the (*a*) 'short bond' and (*b*) 'long bond' ^{19}F neighbours.

More symmetrically arranged ENDOR lines were found around ν_F of ^{19}F at 13.2 MHz. Lines of the 24 second-shell ^{19}F ligands (F(II) ligands) are anticipated. Figure 4 shows the angular dependence, which is complicated because many lines overlap. It was not possible to analyse them fully for all m_S transitions. The solid lines in figure 4 are calculated for the $m_S = -5/2$ second-shell ^{19}F ENDOR lines, assuming $T_\parallel = 1.125$ MHz, $T_\perp = -0.562$ MHz and taking the line connecting the second-shell F and Mn^{2+} as the orientation of the SHF principal axis. Good agreement is found, except for the observation that the ENDOR lines appear to be split into doublets. In contrast to the splitting of the 'first-shell' neighbours, this splitting is not caused by crystal misalignment. It shows up particularly clearly around 16 MHz and 11.5 MHz (see figure 4). The magnetic field is parallel to the SHF axis of two F(II) ligands for $\phi = 25.2°$ from [100] in the (110) rotation plane, and perpendicular to it for 19.5° and 35.3° from [100]. The corresponding extrema in the ENDOR frequencies are clearly seen in figure 4. An analysis demonstrated that the doublet splitting is caused by the fact that the 24 ligands of the second shell are split into two subshells, which slightly differ in the SHF interactions. Assuming the SHF axes to be the connection lines to Mn^{2+} for both subshells, we obtain: $T_\parallel(II_0) = 1.101$ MHz, $T_\perp(II_0) = -0.551$ MHz, $T_\parallel(II_i) = 1.152$ MHz, $T_\perp(II_i) = -0.576$ MHz. The uncertainties are about ±3 kHz.

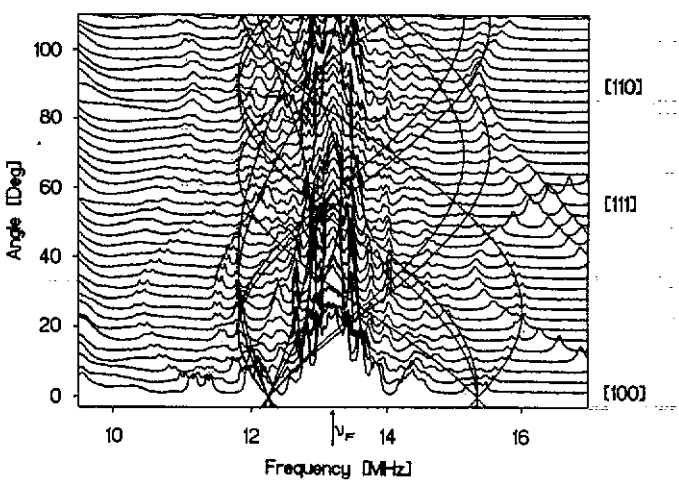

Figure 4. Angular dependence of ^{19}F ENDOR lines for rotation of the magnetic field in a {110} plane for second-shell ligands ($H_0 = 339$ mT, $T = 5$ K) The solid lines are calculated for the $m_S = -5/2$ transitions (see text).

The ENDOR lines of the second shell provide also an additional key for the understanding of the EPR spectra. Selective participation of m_S states is observed if ENDOR measurements are not performed so as to set H_0 into the $m_I = 1/2$ HF group, where the higher-order splittings (cf equation (2)) are small and all Δm_S transitions are saturated simultaneously. This is shown in figure 5 for the magnetic field oriented along [100]. Six lines ($m_S = 5/2$ to $-5/2$) from the eight fluorines whose SHF axes are nearly parallel to H should be expected symmetrically around ν_F, and another six lines, with half the splitting, from the remaining sixteen ^{19}F for which the field is nearly perpendicular to the SHF axes. In the experiment, however, the lines from the positive or the negative m_S states dominate, depending on the field position inside the ^{55}Mn HF group. When setting the magnetic field in positions 1 or 4 of figure 5(*a*) ('outer' parts of the ^{55}Mn HF group), it is mainly the ENDOR lines

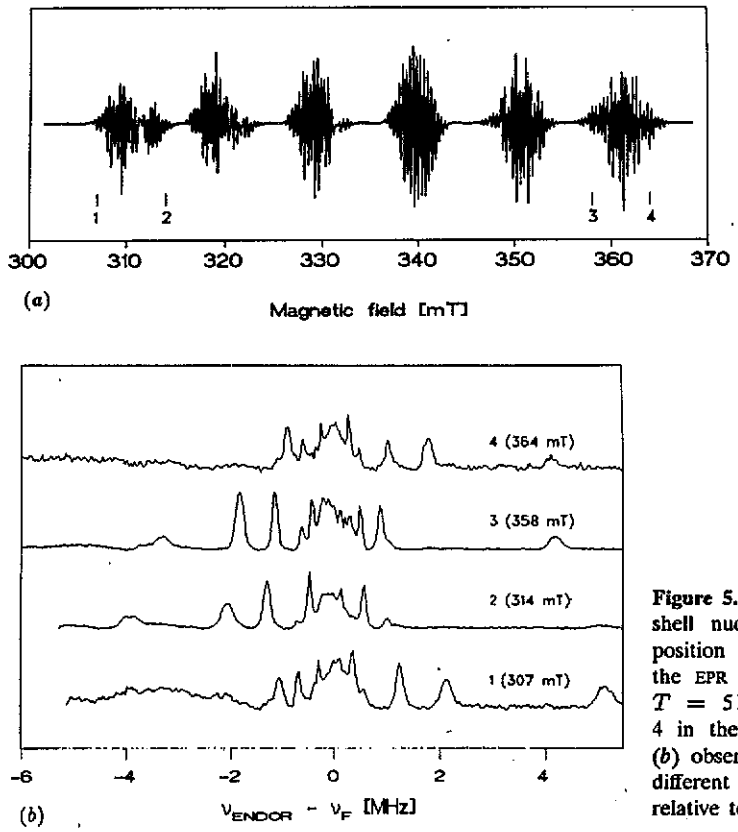

Figure 5. ENDOR pattern of second-shell nuclei as a function of the position of the magnetic field in the EPR spectrum for $H_0 \| [100]$ at $T = 5$ K. (*a*) Field positions 1–4 in the EPR spectrum (see text), (*b*) observed F(II) ENDOR lines for different magnetic field positions relative to ν_F.

of the 'parallel' F(II) nuclei that show up at $\nu_{ENDOR} > \nu_F$ and the 'perpendicular' ones at $\nu_{ENDOR} < \nu_F$ for the $m_S = -5/2$, $-3/2$ and $-1/2$ states (the so-called 'sum frequencies') (Seidel 1961). The opposite is observed if the magnetic field is set to positions 2 and 3 ('difference frequencies'). This is seen in figure 5(*b*), where the ENDOR frequencies are plotted relative to ν_F, which changes if H is changed. In first-order perturbation theory we have

$$\nu_{ENDOR\,\|,\perp} = h^{-1}|\nu_F - T_{\|,\perp} m_S| \tag{6}$$

which explains the observation taking into account the signs of m_S and $T_{\|}$ or $T_{\perp}$, respectively.

These results are in complete accordance with the field positions of different $\Delta m_S = \pm 1$ transitions calculated from equation (2) assuming $a = 0$ (no cubic field splitting) for different values of ^{55}Mn m_I. For the magnetic field positions 1 and 4, negative m_S states are selected; for positions 2 and 3, positive m_S states contribute to the ENDOR transitions. This shows that one finds appreciable higher-order effects in the EPR spectrum, but that the spectrum does not contain the superposition of another Mn^{2+} centre.

Unfortunately, ENDOR could only be observed at very low temperatures. Figure 6 shows that the ENDOR line intensity vanished completely around 9 K. Therefore, we could not follow the transition from the low-temperature configuration to the cubic high-temperature configuration using ENDOR. This result is in marked contrast to

ENDOR observations of Mn^{2+} in CaF_2 up to 50 K (Schön 1992) or in $RbCdF_3$ below and above the structural phase transition at $T = 124$ K (Studzinski *et al* 1986). The observations indicate that the structural instability may be a consequence of lattice dynamics effects which shorten the nuclear spin–lattice relaxation time so much, that ENDOR transitions can no longer be observed.

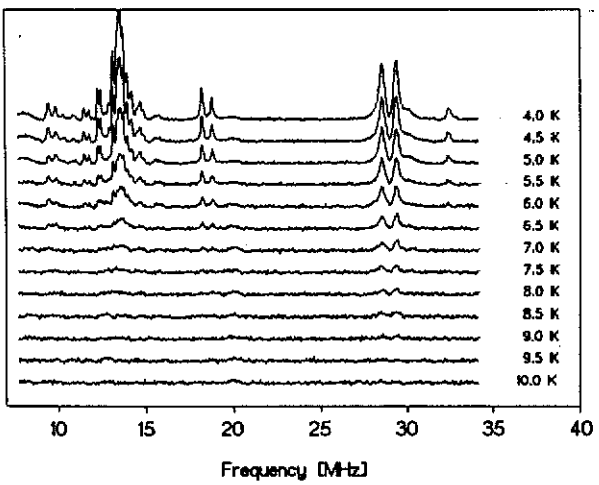

Figure 6. Temperature dependence of ^{19}F ENDOR lines in BaF_2:Mn.

5. Discussion

Since $|T_\perp| = \frac{1}{2}|T_\parallel|$, the second-shell F have no isotropic SHF interaction. Their SHF axes are the connection lines to the central Mn^{2+}. Their anisotropic SHF interaction can thus be interpreted in terms of the classical point dipole–dipole interaction (Spaeth and Seidel 1969, Spaeth 1992):

$$|T_\perp| = (\mu_0/8\pi)g\beta g_N\beta_N 2R^{-3}. \tag{7}$$

From $T_\perp(II_0)$ one obtains $R_1 = (513 \pm 1)$ pm, from $T_\perp(II_i)$, $R_2 = (505 \pm 1)$ pm. Note that R_2 is clearly smaller than the regular distance Ba^{2+}–F(II), which is 514 pm. The following obvious conclusions can be drawn from this.

(*a*) The ENDOR lines around ν_F really originate from the fluorines of the second shell. Therefore the two groups of lines with larger SHF constants belong to the nearer neighbours.

(*b*) The Mn–F(II) distances are smaller than in the regular lattice. Certain lattice contraction seems to occur around the small Mn^{2+} ion replacing Ba^{2+}.

It is also important to note that the ENDOR 'line splitting' occurs for the lines of those F(II) ligands whose positions have inversion symmetry with respect to the Mn^{2+} site (e.g. for the two nuclei in the (110) plane for which the magnetic field becomes parallel to the SHF axes at an angle of 25.2°). This means an opposite

lattice relaxation to a larger (respectively, shorter) distance for these pairs. This has an interesting consequence for the structural changes of the 'first shell'. The near neighbours related to each other by inversion symmetry in the undistorted lattice must relax in different ways in order to result in different distances of the corresponding second-shell ligands. The situation is shown in figure 7, in which the ligands I_i move 'inwards', the ligands I_0 'outwards'. The ligand II_i is then expected to be closer than II_0.

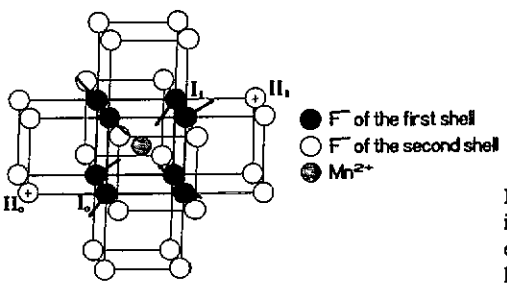

Figure 7. First and second shells of fluorines in BaF_2:Mn. The two nuclei marked by + are equivalent in the {110} plane of the undistorted lattice (see text).

The ENDOR experiments showed the existence of (111) shells, one with larger and the other with smaller SHF interactions, confirming the EPR analysis of Badalyan *et al* (1986). We would associate the larger SHF interaction with the four ligands I_i, tetrahedrally coordinated about Mn^{2+}, and the smaller ones with the tetrahedron of I_0. The values for the second shell indicate that either all eight nearest F neighbours have relaxed inwards, I_i relaxing more then I_0, or the latter have more or less retained their lattice positions while the four I_i have moved in. From the value of $R_1 = 513$ pm, the latter picture also seems plausible.

This situation can, of course, result from a relaxation of all eight neighbours inwards due to the small ionic radius of Mn^{2+}, upon which four neighbours move further in and four again shift outwards. Such a behaviour is suggested by theoretical calculations of Barriuso *et al* (1991), in which the isotropic SHF constant is calculated as a function of ligand distance. According to this calculation for Mn^{2+} in BaF_2, the nearest ligands are 224 pm and the further ones are 250 pm away from Mn^{2+}; in both cases relaxed inwards compared with the 268 pm of the regular lattice distance. The SHF constants, determined here more precisely using ENDOR, hardly change these theoretical values. An estimate yields 224 and 252 pm, respectively. However, it remains to be calculated whether the relaxation of the second-shell fluorines found experimentally is consistent with these theoretical results for the inner neighbours based solely on their Fermi contact term. The high precision of the second-shell distances should allow a very good test of the interpretation of the near-neighbour SHF data by Barriuso *et al*.

Using the SHF constants given above, we calculated a predicted EPR spectrum, including the forbidden transitions (Richardson *et al* 1971). The result which is shown in figure 2(*b*) for the ^{55}Mn $m_I = 1/2$ group only depends critically on the relative magnitudes of the cubic field splitting and the Mn hyperfine splitting (including higher-order terms) and on the linewidths. Satisfactory agreement with the whole spectrum observed in the experiment can be obtained using $A_{Mn} = -100 \times 10^{-4}$ cm^{-1} and a linewidth of 0.2 mT. However, a small but finite fine-structure constant $a = 1.7 \times 10^{-4}$ cm^{-1} has to be included. Otherwise, the 19 lines found experimentally

for ^{55}Mn, $m_I = 1/2$ and $H \parallel [100]$, are not explainable, as one would obtain only 17 lines (see figure 2(*b*)).

A cubic fine-structure constant $a \neq 0$ differs from the findings for BaF_2:Mn at room temperature where $a = 0$ is observed (Richardson *et al* 1972) but is not in contradiction with the tetrahedral symmetry, where the same crystal field term occurs in the spin Hamiltonian (1) with $a_{\text{Tetrahedron}} = a_{\text{Cube}}/2$ for an otherwise unchanged situation. If the difference is due to the reduced Mn–F distance (a varies with the fifth power of the distance), or due to a dynamical averaging in the RT spectra, or (if their resolution is too poor to detect such a small splitting) cannot be decided at the moment. The unusually large linewidth of the SHF structure of Mn^{2+} of BaF_2 compared with that in other fluorites may be a further indication that it is a dynamic process occurring here and causing the instability observed.

6. Conclusions

We have shown that Mn^{2+} substituting for Ba^{2+} in BaF_2 experiences a highly symmetric local instability, resulting in two tetrahedral groups of four fluorines each with different distances from the Mn^{2+} ion. We have thus essentially confirmed the interpretation of the low-temperature EPR spectrum by Badalyan *et al* (1986). However, the ENDOR data on the second-shell F neighbours in particular allowed us to derive a more exact picture of the local structure at low temperatures.

Acknowledgments

One of us (VAV) is indebted to the Humboldt foundation for a grant which enabled him to work in Paderborn. We thank A Hofstaetter for many helpful discussions and F Schoen for some ENDOR data.

References

Badalyan A G, Baranov P G, Vikhnin V S and Khramtsov V A 1986 *Sov. Phys.–JETP Lett.* **44** 110
Barriuso M T, Baranov P G and Moreno M 1991 *Radiat. Eff. Defects Solids* **119 - 121** 177
—— 1971 *Phys. Rev.* B **6** 1065
Richardson R J, Lee S and Menne T J 1972 *Phys. Rev.* B **4** 3837
Schoen F 1992 private communication
Seidel H 1961 *Z. Phys.* **165** 218
Spaeth J M 1992 *Appl. Magn. Reson.* at press
Spaeth J M and Seidel H 1971 *Phys. Status Solidi* **46** 323
Studzinski P and Spaeth J M 1986 *Phys. Status Solidi* b **136** 735
Zaripov M M, Kaibiyainen V K, Meiklyar V P and Falin M L 1975 *Sov. Phys.–Solid State* **17** 1101